European Journal of Orthodontics, 2021, 86–93
doi:10.1093/ejo/cjaa018
Advance Access publication 23 March 2020

Original article

A pilot study to investigate the histomorphometric changes of murine maxillary bone around the site of mini-screw insertion in regenerated bone induced by anabolic reagents

Preksa Keo[1,4], Yoshiro Matsumoto[1], Yasuhiro Shimizu[1], Shigeki Nagahiro[2,4], Masaomi Ikeda[3], Kazuhiro Aoki[4] and Takashi Ono[1]

Departments of [1]Orthodontic Science, [2]Pediatric Dentistry/Special Needs Dentistry, [3]Oral Prosthetic Engineering and [4]Basic Oral Health Engineering, Graduate School of Medical and Dental Sciences, Tokyo Medical and Dental University, Tokyo, Japan

Correspondence to: Kazuhiro Aoki, Department of Basic Oral Health Engineering, Graduate School of Medical and Dental Sciences, Tokyo Medical and Dental University, 1-5-45 Yushima, Bunkyo-ku, Tokyo 113-8549, Japan. E-mail: kazu.hpha@tmd.ac.jp

Summary

Objective: The objective of this study was to investigate the histomorphometric changes around the site of mini-screw insertion in the regenerated bone which was induced by an anabolic-injection method using both anabolic peptide and bone morphogenetic protein 2 (BMP-2).

Methods: Twenty-seven eight-week-old C57BL/6J male mice were used. Some mice received submucosal co-injections of anabolic peptide and BMP-2 just in front of the maxillary first molar. Screw insertion was then performed 4 weeks after injection. All mice underwent a weekly *in vivo* micro-focal X-ray computed tomography (μCT) analysis before being sacrificed at week 8. The bone formation activity was evaluated using fluorescent labelling in the undecalcified sections. The analyses, including screw insertion, were performed in the frontal plane, in front of the site of screw insertion.

Results: Reconstructed μCT images revealed that the co-injection of anabolic reagents could lead to a gradual increase in the bone mineral density (BMD) of the injection-induced thickened bone by week 8. Both radiological and histomorphometric analyses indicated that screw insertion did not have any deleterious effects on either the BMD or the bone formation activity of the induced bone. Furthermore, the injection of anabolic reagents also led to an increase in the BMD of the underlying maxillary bone at the injection site.

Conclusion: Our histomorphometric analyses suggest that performing such anabolic injection to thicken bone could stimulate bone formation in the basal bone as well as in the induced bone. Similar augmentation of bone formation could be obtained even after subsequent screw insertion at the site of the induced bone.

Introduction

The mini-screw plays a pivotal role in orthodontic treatment (1, 2). It acts as a skeletal anchor preventing undesired tooth movement and also assists in skeletal modification (3–6). However, there are several problems that hinder successful mini-screw insertion (7). Anatomical limitations, such as insufficient bone volume or the thickness of the cortical bone, especially the edentulous space, may lead to poor primary stability of the mini-screws (8–10). Although a larger diameter improves the primary stability, thick mini-screws cannot be inserted in the tight spaces between roots (9, 11). This leads to the occurrence of iatrogenic root injury and screw fracture. Several other factors might contribute to such mini-screw failure. Factors such as low bone mineral density (BMD) greatly influence the final outcome of mini-screw insertion (12). Different parts of the jaws have different mineral densities (13). For instance, the posterior part of the maxilla has a low BMD and is therefore likely to demonstrate screw loosening over time (14). Moreover, individuals who suffer from systemic diseases, such as type-I diabetes or postmenopausal women, have a low BMD (15, 16). In clinical practice, however, mini-screws can be placed in other parts of the jaw, such as the hard palate, to avoid causing root injury or avoid placement in tight spaces (17–20). This requires the careful planning of orthodontic mechanics and it is usually associated with other problems such as patient discomfort. Various extra-oral appliances can be used to reinforce the anchorage, such as headgear (21). This method relies heavily on patient compliance which might not always produce a desirable outcome (22). Thus, a different approach is necessary to facilitate mini-screw insertion.

We recently established an efficient method for thickening the maxillary bone by injecting anabolic materials to form additional bone at the site where thick bone is necessary; this method might be useful for solving the above-mentioned anatomical limitations and the problem of low BMD (23). The reagents used for injection include anabolic peptide and bone morphogenetic protein 2 (BMP-2). The anabolic peptide is originally designed from the binding site of the receptor activator of NF-κB ligand (RANKL) on osteoprotegerin, thereby inhibiting the osteoclast activity (24). Recently, this RANKL-binding peptide OP3-4 has been recognized as a stimulator of osteoblast differentiation and bone formation (25–27). The other reagent is BMP-2, which has been used to induce ectopic bone due to its great osteogenic potential. The combination of BMP-2 and the peptide produces a synergistic effect. This has been proven to be effective in stimulating bone formation in various animal models. The synergistic effect of the two materials induces sufficient bone formation to cover the critical-sized defect in the calvaria-defect model, while also improving BMP-2-induced osteogenesis in the tooth extraction socket (25, 28). We therefore hypothesized that this anabolic-injection method might improve the BMD and increase the thickness of the bone at the injection site, where additional thickness is necessary for screw insertion. Thus, the purpose of this study was to investigate the histomorphometric changes around the site of mini-screw insertion in the regenerated bone which was induced by an anabolic-injection method using both anabolic peptide and BMP-2.

Materials and methods

Animals

Twenty-seven seven-week-old C57BL/6J male mice were purchased from NIPPON CLEA (Tokyo, Japan). All animals were given a week to adapt to a 12-hour dark/light cycle under constant temperature (22 ± 1°C) with *ad libitum* access to food and water. All of the experimental procedures were approved by the Animal Care and Use Committee of Tokyo Medical and Dental University (Tokyo, Japan, authorization numbers: A2017-280C7, A2018-102A, A2019-096A).

Experimental design and surgical procedure

Eight-week old mice were subcutaneously anaesthetized with a mixed solution consisting of medetomidine hydrochloride (0.75 mg/kg; Dormitol, Zenoaq, Fukushima, Japan), Midazolam (4 mg/kg; Midazolam®, Sando, Yamagata, Japan) and Butorphanol (5 mg/kg; Vetorphale, Meiji Seika Pharma Co., Ltd, Tokyo, Japan). They recovered after the subcutaneous injection of atipamezole (0.75 mg/kg; Antisedan, Zenoaq), which is an antagonist of medetomidine hydrochloride. Some mice were randomly selected to receive a 4-µl submucosal injection of a mixture of gelatin hydrogel (pI9; provided by Prof. Y. Tabata, Department of Biomaterials, Kyoto University, Kyoto, Japan), BMP-2 (provided by Bioventus LLC, Durham, North Carolina, USA), and anabolic peptide (OP3-4; Atlantic peptides, Lewisburg, Pennsylvania, USA) in front of the right maxillary first molar (incisor-first molar diastema of the right maxilla) using a 26-gauge Hamilton needle and a 25-µl Hamilton syringe, as previously described (Figure 1B) (23). Due to the delicate nature of the mucosal tissue, the injection site, where the needle was inserted, had to be placed approximately 2.0 mm away from bone formation site, namely where the screw was to be placed. At four weeks after injection, some mice were randomly chosen for pure titanium screw insertion (diameter: 0.8 mm; length: 1.5 mm; Matsumoto Industry Co., Ltd, Chiba, Japan) either inside the newly formed bone or the maxillary bone, as previously mentioned with some modifications

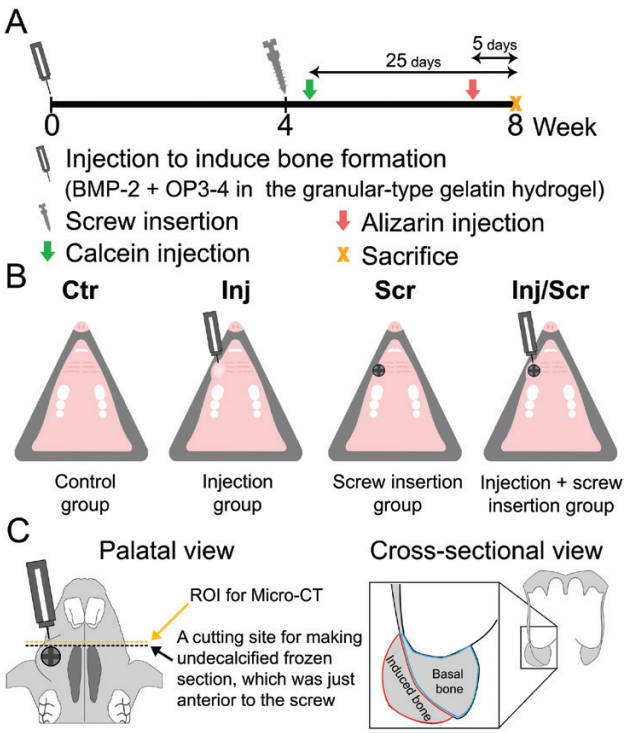

Figure 1. The experimental design. (A) The schedule for the injection of bone anabolic materials, screw insertion, and fluorescent labelling. (B) A schematic representation of the experimental groups. (C) The regions of interest (ROIs) for analysing the micro-CT (µCT) images and undecalcified sections. Both analyses were performed in the areas of induced bone and the basal bone, as shown in the right panel.

(Figure 1A) (29). Then, the mice were divided into the following four groups: the control group (Ctr; n = 6), the injection group (Inj; n = 9), the screw insertion group (Scr; n = 4), and the injection and screw insertion group (Inj/Scr; n = 8) (Figure 1B). Next, two bone labelling agents, Calcein (20 mg/kg; Sigma-Aldrich, St. Louis, Missouri, USA) and Alizarin complexone (20 mg/kg; ALC, Donjindo, Kumamoto, Japan), were administered at 25 and 5 days before sacrifice, respectively (Figure 1A). All mice were sacrificed by cervical dislocation under anaesthesia at week 8. The craniums deprived of the mandibles were carefully dissected. The samples were then thoroughly washed by phosphate buffered saline (PBS) before being submerged in 10% PBS-based formaldehyde fixative (pH 7.4) for 48 hours at 4°C under constant shaking motion. All samples were then washed and stored in PBS for further analyses, as described previously (23).

Radiological assessment

From the second week after injection, *in vivo* micro-focal X-ray computed tomography (μCT) was performed on a weekly basis. Three-dimensional (3D) reconstruction images of the maxillae were captured by *in vivo* μCT (R_mCT2 SPMD, Rigaku, Tokyo, Japan; 90 kV and 160 mA within a 10-mm field of view). All 3D data were first reconstructed under the same configurations and then were arranged in a way that the occlusal plane was parallel to the floor and balanced between left and right. The contact point between the first and second molar was used as a reference point throughout this analysis so that the same region of interest (ROI) for BMD analyses could be selected each time. Next, we divided the bone into two parts, induced bone and basal bone, and the border of these two regions was determined by the shape of basal bone on μCT images (Figure 1C). We also used fluorescence microscopy to recognize the induced bone and basal bone. In order to observe the changes of the induced bone and exclude the effects of the radiological artefact of the screw, the frontal plane 4.2 mm anterior from the contact site of the first and the second molars and 0.2-mm thickness, anterior to screw placement was chosen as the ROI for a BMD analysis (Figure 1C). Based on the ROI shown here, the bone thickness at week 8 was calculated by dividing the total bone volume by the total bone surface, which were measured based on the μCT images shown above, and multiplied by two. All μCT analyses were performed using the TRI/3D-BON imaging software program (Ratoc System Engineering, Tokyo, Japan).

Histological assessment and bone histomorphometry

The maxillae were cut just anterior to the screws using a saw microtome (SP1600; Leica Biosystems, Nussloch, Germany) under a constant flow of water (Figure 1C). The anterior portions of the maxillae were then embedded in SCEM compound (Section-Lab Co. Ltd, Hiroshima, Japan) and frozen into blocks at −100°C in a freezing machine (UT2000F; Leica Microsystems, Tokyo, Japan). The undecalcified frozen blocks were then cut into slices measuring 5 μm in thickness using a microtome (CM3050sIV; Leica Biosystems) and then were retrieved by adhesive Kawamoto film (Cryofilm type 2C [9], Section-Lab, Co., Ltd), as described previously (23). Thereafter, both von Kossa and tartrate-resistant acid phosphatase staining were applied to identify the calcified tissue and osteoclasts, respectively, as described previously (30). The fluorescence-labelled sections were observed under a fluorescence microscope (FSX100; Olympus, Tokyo, Japan). The mineral apposition rate (MAR) was calculated by measuring the inter-labelled distance between a Calcein-labelled line (green colour) and an Alizarin-labelled line (red colour), and divided by the 20-day interval. The bone formation rate (BFR) (area reference) was calculated by multiplying the mineralizing surface (MS) by the MAR and divided by the bone area, as described previously (31). We divided the basal bone into outer and inner portions. The outer portion was approximately 200 μm from the outer border, and the rest of the basal bone was regarded as the inner portion. The eroded surface and osteoclast number per bone surface was calculated by dividing the total eroded surface and number of osteoclasts by the trabecular surface of the basal bone, respectively (31).

Statistical analyses

All results are presented as the mean ± standard deviation (SD). All statistical analyses were carried out using SPSS ver. 22.0 (IBM, Chicago, USA). Sample size calculations were done based on the pilot study and a previous study which performed similar comparisons (23) using the formula noted below:

Sample size calculation:

$$N = 2(Z_{\alpha/2} + Z_{\beta})^2 \mathrm{SD}^2 / \Delta^2 \sqrt{2}$$

where $Z_{\omega/2}$: significance = 5%; Z_{β}: power = 80%; SD: standard deviation; Δ: the difference between the mean value.

$$\begin{aligned} N &= 2(Z_{\alpha/2} + Z_{\beta})^2 \mathrm{SD}^2 / \Delta^2 \\ &= 2(1.96 + 0.84)^2 20^2 / 50^2 \\ &= 3.36 \end{aligned}$$

We also assumed that $0.05 < P < 0.1$ indicated edge cases of significance or were highly suggestive of significance according to the statement by the American Statistical Association (32, 33). The difference between the mean value and SD was determined by the pilot and the findings of a previous study (23). Non-parametric analyses were performed using the Wilcoxon signed-rank test, the Wilcoxon rank sum test with/without Bonferroni correction ($P < 0.05$), while parametric analyses were performed using the t-test with/without Bonferroni correction ($P < 0.05$). The significance level was modified by the number of comparisons using the Bonferroni correction formula noted below:

Formula of Bonferroni correction:

$$\alpha = 0.05/[\beta(\beta - 1)/2]$$

where α: significance level; β: number of groups.

Results

Anabolic injection regenerated bone at the injection site and thickened the bone of the maxilla at week 8

Anabolic-injection-induced bone began to form at week 2; however, the radio opacity was relatively low (Figure 2A). At this point, the average BMD of the induced bone was approximately 265 mg/cm^3 (Figure 2B). From week 3, the bone progressively started to take shape, reaching an average BMD of approximately 565 mg/cm^3 at week 4, which was twice the average BMD observed at week 2 (Figure 2B). By week 5, the border between the induced bone and the basal bone became less distinguishable since the white region, which represents a higher BMD (>700 mg/cm^3) seemed to fuse into a single block. The induced bone gradually mineralized, peaking at week 8 at approximately 785 mg/cm^3, which was approximately 3-fold the BMD observed at week 2 (Figure 2B). The induced bone was compact

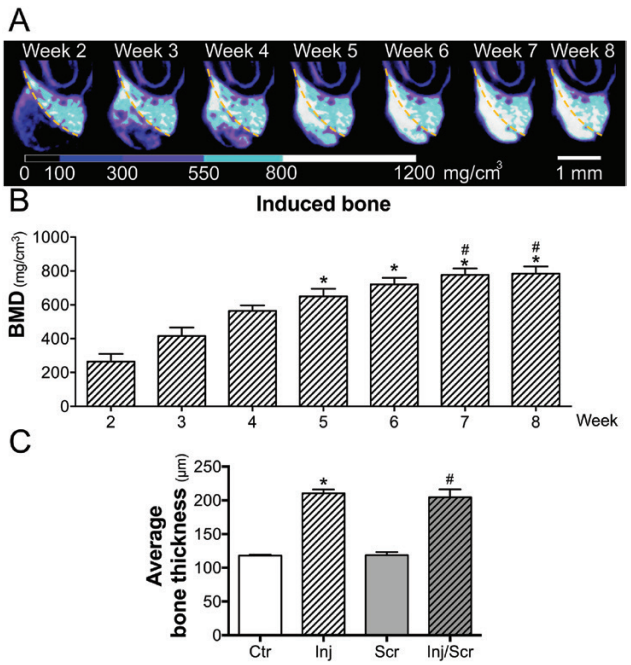

Figure 2. Changes in the bone mineral density (BMD) of the anabolic-injection-induced bone and the effects of anabolic injection on bone thickness. (A) Changes in the *in vivo* μCT reconstruction images up to 8 weeks after anabolic injection. The orange dotted lines represent the border of the basal bone and the induced bone. (B) The time-course study of the BMD of induced bone. The Wilcoxon signed-rank test was performed with Bonferroni correction ($P < 0.05$). $^{*}P < 0.05$ versus week 2, $^{\#}P < 0.05$ versus week 4. (C) The average bone thickness at week 8. Ctr, control group; Scr, screw insertion group; Inj, injection group; Inj/Scr, injection and screw insertion group. The Wilcoxon rank sum test was performed with Bonferroni correction ($P < 0.05$). $^{*}P < 0.05$ versus the Ctr group, $^{\#}P < 0.05$ versus the Scr group. The data are shown as the mean ± SD.

and appeared as a cortical-like structure (Figure 2A). The average bone thickness at week 8 clearly showed a significant increase in both groups that received anabolic injections (Inj and Inj/Scr) in comparison to the non-injected groups (Ctr and Scr) (Figure 2C).

Screw insertion had no deleterious effects on BMD in the induced bone

To investigate the changes in the BMD of the newly formed bone (induced bone) after the subsequent screw insertion, we performed *in vivo* μCT analyses comparing the induced bone of the Inj group to that of the Inj/Scr group at weeks 4 and 8, and found no difference in the BMD of the induced bone between the two groups (Figure 3A). The observance of fluorescence images of undecalcified sections revealed distinct Calcein- and Alizarin-labelled lines that appeared similarly in both injected groups (Figure 3B and 3C). The distance between the two labelled lines was also similar in the two groups (Figure 3C). Quantitative analyses of MAR and BFR, which show the bone formation activity of each osteoblast and the BFR from 25 to 5 days before sacrifice, respectively, indicated that the bone formation activity in the induced bone was not reduced by screw insertion for at least 20 days (days 3 to 23) after screw insertion (Figure 3B and 3C).

Anabolic injection increased the BMD of the basal bone adjacent to the induced bone

At week 4, there were visible differences in the basal bone between the injected groups (Inj and Inj/Scr) and the non-injected groups (Ctr

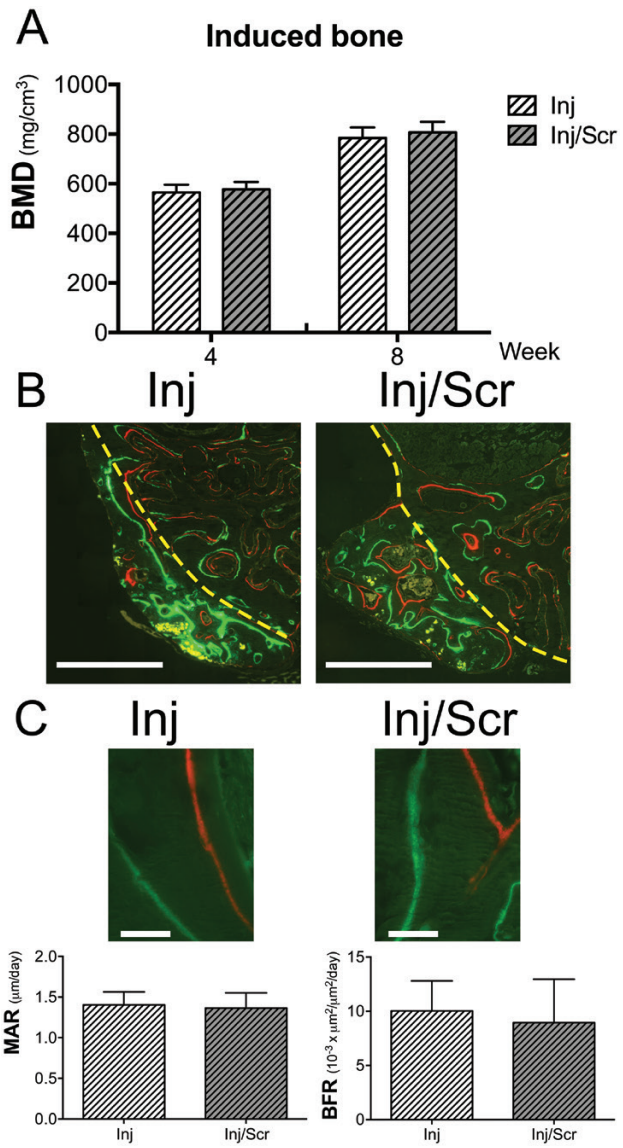

Figure 3. The induced bone was not affected by screw insertion. (A) The BMD of the induced bone of the Inj and Inj/Scr groups at weeks 4 and 8. (B) Fluorescence images of the induced bone. Yellow dotted lines separate the induced bone from the basal bone. Scale bar = 500 μm. (C) Fluorescence images of inter-labelled lines of the induced bones of the Inj and Inj/Scr groups and quantitative data on the bone formation activity of the induced bone. The data are shown as the mean ± SD. The Wilcoxon rank sum test was performed. Scale bar = 25 μm.

and Scr), since the white region, which represented a high BMD (as shown in the colour bar of Figure 4A), was more clearly evident in the injected groups. Interestingly, the high BMD region shown in white in the injected groups (Inj and Inj/Scr) was more prominent in the basal bone adjacent to the induced bone (Figure 4A). As shown in Figures 2C and 3, the anabolic injection increased the bone thickness and led to active bone formation in the induced bone. We thought that this active bone formation in the induced bone might influence the basal bone and increase the BMD (Figure 4B). The active bone formation of induced bone can also be observed using von Kossa staining, which revealed extensive mineralization of the whole induced bone (Figure 5A). As a result, the total bone area of injected groups was found to significantly increase (Figure 5B and Supplementary Figure 1).

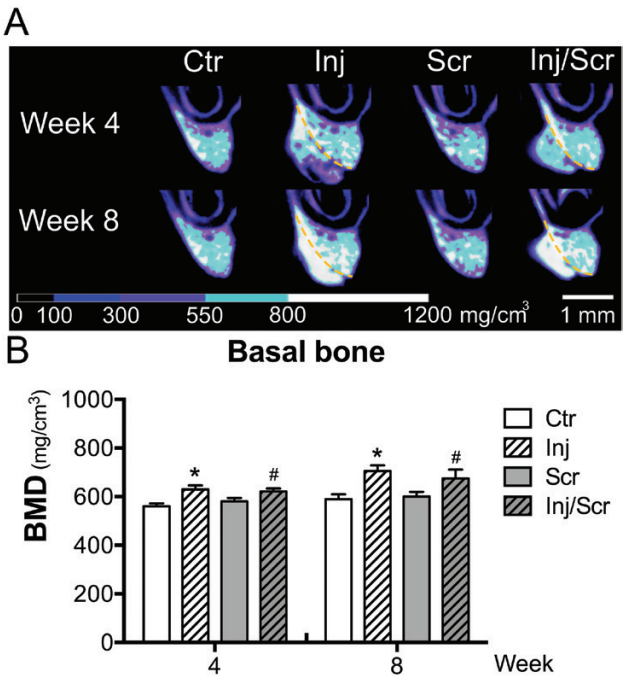

Figure 4. The induced bone might increase the BMD of basal bone. (A) µCT images of each group at weeks 4 and 8. Scale bar = 1 mm. (B) The BMD of the basal bone. The data are shown as the mean ± SD. The Wilcoxon rank sum test with Bonferroni correction ($P < 0.05$). $^{*}P < 0.05$ versus the Ctr group, $^{\#}P < 0.05$ versus the Scr group.

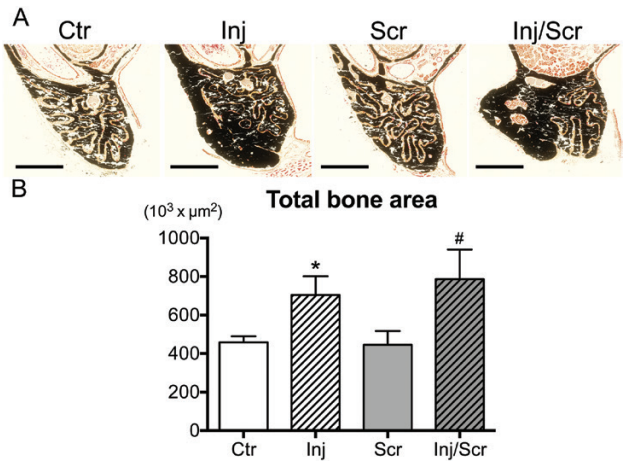

Figure 5. von Kossa staining revealed an increased calcification area of bone in the injected groups. (A) von Kossa-stained images of the maxilla bone. A cortical bone structure appeared in the injected groups. Scale bar = 500 µm. (B) Total bone area. The data are shown as the mean ± SD. The *t*-test with Bonferroni correction ($P < 0.05$) was performed. $^{*}P < 0.05$ versus the Ctr group, $^{\#}P < 0.05$ versus the Scr group.

To further clarify the influence of the induced bone on the basal bone, we first observed fluorescence-labelled images and found that the basal bones of the injected groups were partly affected along the outer border (Figure 6A). Thus, we divided the basal bone into outer and inner portions, as described in Materials and methods. Quantitative measurements clearly showed the BFR value of the outer portions of both injected groups, which was calculated from MAR and MS/BS, to be greater in comparison to those of the outer portions of the non-injected groups, while the MAR and BFR values of the inner portions did not differ among the groups to a statistically significant extent (Figure 6B and Supplementary Figure 2). The resorption parameters, eroded surface and osteoclast number per bone surface, did not differ among the groups to a statistically significant extent (Figure 6C and Supplementary Figure 3).

Discussion

In orthodontic treatment, secure mini-screw insertion mainly relies on primary stability, while the primary stability itself relies greatly on the thickness of the cortical bone (9, 10). Our study provides the first evidence showing the effects of subsequent screw insertion after inducing bone formation using anabolic injections. We previously demonstrated that a protein/peptide combination (using the same injectable gel carrier as used in this study) promoted bone formation in the mouse maxilla (23). Usually, the size of the regenerated bone induced by BMP-2 is carrier-size dependent, as we demonstrated in our previous study. Since the injectable carrier was a granular-type carrier measuring 20-µm in diameter, the regenerated bone induced by BMP-2 alone could not induce bone thickening at the injection site, while co-injection with the anabolic peptide was able to induce bone thickening, while also increasing the height of the jaw bone as we observed in the present study (Figures 2C and 4A) (23). Thus, we could confirm the reproducibility of our anabolic-injection method to thicken bone at a desired location with only a single injection.

The BMD at the mini-screw site is another important factor for successful mini-screw placement (14). For example, the posterior maxilla, which has a relatively low BMD, is not a favourable place for mini-screw insertion (13). Screw migration is known to occur less frequently in bone with a high BMD (34). Furthermore, patients with a low BMD might be prone to mini-screw failure (15, 16, 35). In order to prevent such events in patients with a low BMD, the BMD should be increased for successful mini-screw insertion. Actually, *in vivo* µCT revealed a gradual increase in the BMD of the induced bone by week 8 (Figure 2A and 2B), and our anabolic-injection method led to an increase of the BMD in the basal bone at the injection site, as well as a gradual increase in the BMD of the induced bone (Figures 2 and 4A, 4B). Thus, our study suggests that the anabolic-injection method using BMP-2 and an anabolic peptide might have the potential to overcome the anatomical limitations that may lead to failure after mini-screw placement.

The results showing the increase in the bone formation activity in the basal bone at the injection site might therefore indicate that the anabolic-injection method helps to facilitate successful mini-screw insertion (Figure 6 and Supplementary Figure 2). Since the predrilled guides are not usually used for mini-screw insertion, bone elasticity is known to be important for the direct insertion of the mini-screw (11, 36, 37). As Figure 6 demonstrates, the bone formation increased at the injection site in the outer portion of the basal bone, as well as in the induced bone itself, in comparison to the inner portion of the basal bone. Since the newly formed bone is known to have high elasticity, sites of active formation are also thought to have greater elasticity than sites with low bone formation activity (38). Our data suggest that the injection-induced increase of bone formation could lead to easier mini-screw insertion in comparison to the approach without anabolic injection. A study using bigger animals is necessary to clarify the effects of our anabolic-injection method with regard to the facilitation of mini-screw insertion.

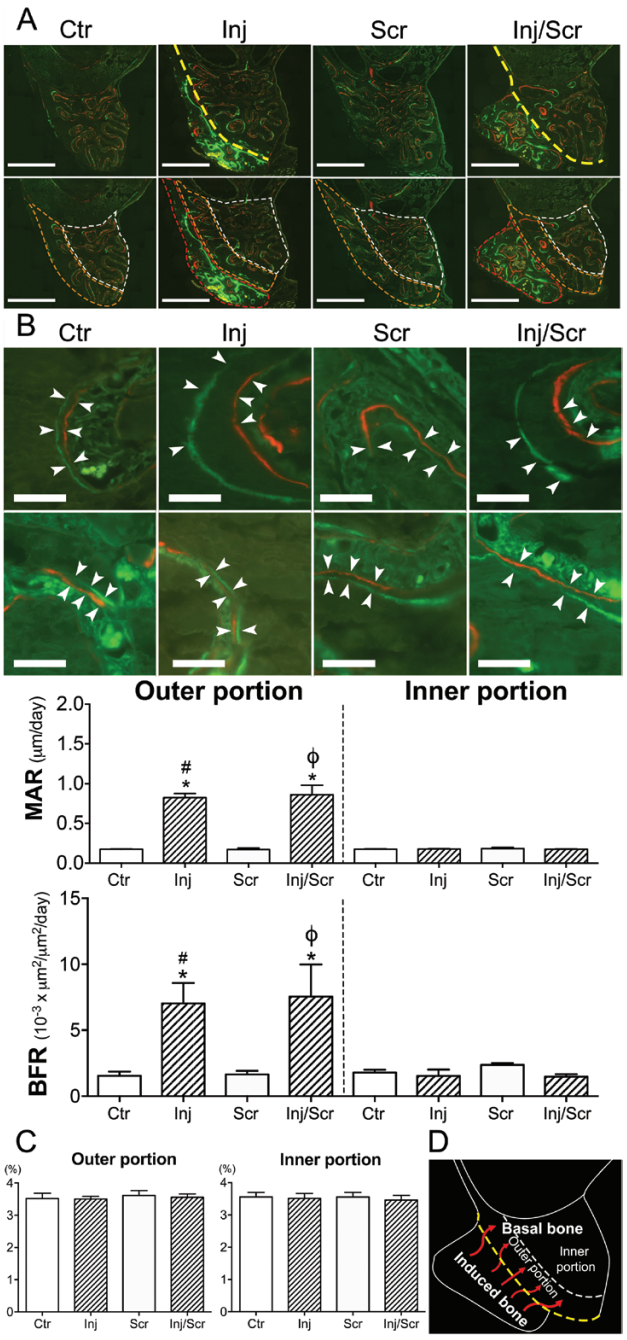

Figure 6. Fluorescence images revealed increased bone formation activity in the outer portions of the basal bone of the groups that received injections and stable bone resorption activity. (A) Fluorescence images of the induced and basal bone. The upper panel shows induced and basal bone separated by yellow dotted lines. The lower panel shows induced bone, with the outer and inner portions of the basal bone separated by red, orange and white dotted lines, respectively. The thickness of the outer portion was 200 μm. Scale bar = 500 μm. (B) Fluorescence images of inter-labelled lines of the outer portions (upper panel) and the inner portions (lower panel) indicated by white arrowheads and quantitative data on bone formation activity of all groups. Scale bar = 25 μm. (C) The eroded surface. (D) A schematic representation of the influence of induced bone on the outer portion in the basal bone. The data are shown as the mean ± SD. The Wilcoxon rank sum test was performed with Bonferroni correction ($P < 0.05$). $^{*}P < 0.05$ versus the outer portion of the Ctr group, $^{\#}P < 0.05$ versus the outer portion of the Scr group, ϕ $0.05 < P < 0.1$ versus the outer portion of the Scr group.

The stimulatory mechanism of bone formation induced by anabolic injection is recognized as a synergistic effect of the RANKL-binding peptide and BMP-2 on bone formation (39). The RANKL-binding peptide stimulates the phosphorylation of Smad1/5 protein, which is downstream in the BMP-2 signalling pathway. Furthermore, the RANKL-binding peptide has been proven to accelerate osteoblast differentiation directly through the surface protein RANKL on osteoblasts (25, 26). These actions induced by the anabolic peptide and BMP-2 could affect the BMD and bone formation activity in the basal bone at the site of the anabolic injection. Further studies are necessary to clarify whether the BMD and bone formation induced by our anabolic-injection method can be maintained at a certain level after the application of loading on the screw.

In summary, our anabolic-injection method increased the bone thickness, BMD, and bone formation activity, even in the basal bone at the injection site. Our results also indicated that similar bone formation was obtained after the subsequent screw insertion, suggesting that our anabolic-injection method might prevent mini-screw failure due to the lack of bone thickness and a low BMD at the site of screw insertion.

Supplementary material

Supplementary data are available at *European Journal of Orthodontics* online.

Supplementary Figure 1. Bone area measurements using von Kossa staining. (A) The von Kossa-stained images of the induced and basal bone. The induced bone, outer, and inner portions of the basal bone were separated by red, orange, and white dotted lines, respectively. Scale bar = 500 μm. The outer portion of the basal bone was defined as described in Materials and methods. (B) The bone area of induced bone. (C) The basal bone area in the outer and inner portions. The *t*-test and *t*-test with Bonferroni correction ($P < 0.05$) were performed for the bone area of induced bone (B) and basal bone (C), respectively.

Supplementary Figure 2. The mineralizing surface in the basal bone. Quantitative data of the mineralizing surface per bone surface (MS/BS) of the outer and inner portions of the basal bone. The data are shown as the mean ± SD. The *t*-test was performed with Bonferroni correction ($P < 0.05$).

Supplementary Figure 3. The osteoclast number using TRAP staining. (A) The osteoclast number per bone surface (N.Oc/BS) in the induced bone. (B) N.Oc/BS in the outer and inner portions of the basal bone. The data are shown as the mean ± SD. The Wilcoxon test and Wilcoxon with Bonferroni correction ($P < 0.05$) were performed for the induced bone (A) and basal bone (B), respectively.

Funding

This work was supported by the Japan Society for the Promotion of Science (15K11344 to Y.M., 19H01068 to K.A.).

Acknowledgements

We would like to extend our sincere appreciation to Dr Yukihiko Tamura, Dr Masud Khan, Dr Hisami Okawara, Dr Masamu Inoue, Dr Yang Shin Sheng, Dr Phyo Thura Aung, and Ms Mariko Takahashi of the Graduate School of Medical and Dental Sciences of Tokyo Medical and Dental University for their great contribution in providing the skills necessary to carry out our research and in

solving technical problems as well as Mrs Akiyama Masako of the Research University Promotion Organization for her guidance in the statistical analyses.

Conflicts of interest

None to declare.

References

1. Lee, J.S., Kim, J.K. and Park, Y.C. (2017) Biomechanical considerations with temporary anchorage devices. In Graber LW, Vanarsdall RL, Vig KWL, Huang GJ (eds.), *Orthodontics—Current Principles and Techniques*. Elsevier, St. Louis, Missouri, pp. 511–568.
2. Proffit, W.R., Fields, H.W.J., Larson, B. and Sarver, D.M. (2019) Contemporary orthodontic appliances. In: Proffit WR, Larson BE (eds.), *Contemporary Orthodontics*. Mosby Elsevier, Philadelphia, PA, pp. 310–351.
3. Upadhyay, M., Yadav, S. and Patil, S. (2008) Mini-implant anchorage for en-masse retraction of maxillary anterior teeth: a clinical cephalometric study. *American Journal of Orthodontics and Dentofacial Orthopedics*, 134, 803–810.
4. Chung, K.R., Kim, S.H., Choo, H., Kook, Y.A. and Cope, J.B. (2010) Distalization of the mandibular dentition with mini-implants to correct a Class III malocclusion with a midline deviation. *American Journal of Orthodontics and Dentofacial Orthopedics*, 137, 135–146.
5. Eissa, O., ElShennawy, M., Gaballah, S., ElMehy, G. and El-Bialy, T. (2018) Treatment of Class III malocclusion using miniscrew-anchored inverted Forsus FRD: controlled clinical trial. *The Angle Orthodontist*, 88, 692–701.
6. Lee, K.J., Park, Y.C., Park, J.Y. and Hwang, W.S. (2010) Miniscrew-assisted nonsurgical palatal expansion before orthognathic surgery for a patient with severe mandibular prognathism. *American Journal of Orthodontics and Dentofacial Orthopedics*, 137, 830–839.
7. Kuroda, S. and Tanaka, E. (2014) Risks and complications of miniscrew anchorage in clinical orthodontics. *Japanese Dental Science Review*, 50, 79–85.
8. Farnsworth, D., Rossouw, P.E., Ceen, R.F. and Buschang, P.H. (2011) Cortical bone thickness at common miniscrew implant placement sites. *American Journal of Orthodontics and Dentofacial Orthopedics*, 139, 495–503.
9. Shah, A.H., Behrents, R.G., Kim, K.B., Kyung, H.M. and Buschang, P.H. (2012) Effects of screw and host factors on insertion torque and pullout strength. *The Angle Orthodontist*, 82, 603–610.
10. Marquezan, M., Mattos, C.T., Sant'Anna, E.F., de Souza, M.M. and Maia, L.C. (2014) Does cortical thickness influence the primary stability of miniscrews? A systematic review and meta-analysis. *The Angle Orthodontist*, 84, 1093–1103.
11. Chen, Y., Kyung, H.M., Gao, L., Yu, W.J., Bae, E.J. and Kim, S.M. (2010) Mechanical properties of self-drilling orthodontic micro-implants with different diameters. *The Angle Orthodontist*, 80, 821–827.
12. Marquezan, M., Osório, A., Sant'Anna, E., Souza, M.M. and Maia, L. (2012) Does bone mineral density influence the primary stability of dental implants? A systematic review. *Clinical Oral Implants Research*, 23, 767–774.
13. Choi, J.H., Park, C.H., Yi, S.W., Lim, H.J. and Hwang, H.S. (2009) Bone density measurement in interdental areas with simulated placement of orthodontic miniscrew implants. *American Journal of Orthodontics and Dentofacial Orthopedics*, 136, 766.e1–12; discussion 766.
14. Chugh, T., Jain, A.K., Jaiswal, R.K., Mehrotra, P. and Mehrotra, R. (2013) Bone density and its importance in orthodontics. *Journal of Oral Biology and Craniofacial Research*, 3, 92–97.
15. Pouresmaeili, F., Kamalidehghan, B., Kamarehei, M. and Goh, Y.M. (2018) A comprehensive overview on osteoporosis and its risk factors. *Therapeutics and Clinical Risk Management*, 14, 2029–2049.
16. Seeman, E. (2013) Age- and menopause-related bone loss compromise cortical and trabecular microstructure. *The Journals of Gerontology. Series A, Biological Sciences and Medical Sciences*, 68, 1218–1225.
17. Bittencourt, L., Raymundo, M. and Mucha, J. (2010) The optimal position for insertion of orthodontic miniscrews. *Revista Odonto Ciência*, 26, 133–138.
18. Ichinohe, M., Motoyoshi, M., Inaba, M., Uchida, Y., Kaneko, M., Matsuike, R. and Shimizu, N. (2019) Risk factors for failure of orthodontic mini-screws placed in the median palate. *Journal of Oral Science*, 61, 13–18.
19. Ludwig, B., Glasl, B., Bowman, S.J., Wilmes, B., Kinzinger, G.S. and Lisson, J.A. (2011) Anatomical guidelines for miniscrew insertion: palatal sites. *Journal of Clinical Orthodontics*, 45, 433–41; quiz 467.
20. Tepedino, M., Cattaneo, P.M., Masedu, F. and Chimenti, C. (2017) Average interradicular sites for miniscrew insertion: should dental crowding be considered? *Dental Press Journal of Orthodontics*, 22, 90–97.
21. Yao, C.C., Lai, E.H., Chang, J.Z., Chen, I. and Chen, Y.J. (2008) Comparison of treatment outcomes between skeletal anchorage and extraoral anchorage in adults with maxillary dentoalveolar protrusion. *American Journal of Orthodontics and Dentofacial Orthopedics*, 134, 615–624.
22. Al-Moghrabi, D., Salazar, F.C., Pandis, N. and Fleming, P.S. (2017) Compliance with removable orthodontic appliances and adjuncts: a systematic review and meta-analysis. *American Journal of Orthodontics and Dentofacial Orthopedics*, 152, 17–32.
23. Uehara, T., Mise-Omata, S., Matsui, M., Tabata, Y., Murali, R., Miyashin, M. and Aoki, K. (2016) Delivery of RANKL-binding peptide OP3-4 promotes BMP-2-induced maxillary bone regeneration. *Journal of Dental Research*, 95, 665–672.
24. Cheng, X., Kinosaki, M., Takami, M., Choi, Y., Zhang, H. and Murali, R. (2004) Disabling of receptor activator of nuclear factor-kappaB (RANK) receptor complex by novel osteoprotegerin-like peptidomimetics restores bone loss in vivo. *The Journal of Biological Chemistry*, 279, 8269–8277.
25. Sugamori, Y., *et al*. (2016) Peptide drugs accelerate BMP-2-induced calvarial bone regeneration and stimulate osteoblast differentiation through mTORC1 signaling. *Bioessays*, 38, 717–725.
26. Ikebuchi, Y., *et al*. (2018) Coupling of bone resorption and formation by RANKL reverse signalling. *Nature*, 561, 195–200.
27. Sone, E., *et al*. (2019) The induction of RANKL molecule clustering could stimulate early osteoblast differentiation. *Biochemical and Biophysical Research Communications*, 509, 435–440.
28. Arai, Y., Aoki, K., Shimizu, Y., Tabata, Y., Ono, T., Murali, R., Mise-Omata, S. and Wakabayashi, N. (2016) Peptide-induced de novo bone formation after tooth extraction prevents alveolar bone loss in a murine tooth extraction model. *European Journal of Pharmacology*, 782, 89–97.
29. Nguyen Vo, T.N., Hao, J., Chou, J., Oshima, M., Aoki, K., Kuroda, S., Kaboosaya, B. and Kasugai, S. (2017) Ligature induced peri-implantitis: tissue destruction and inflammatory progression in a murine model. *Clinical Oral Implants Research*, 28, 129–136.
30. Nagahama, K., Aoki, K., Nonaka, K., Saito, H., Takahashi, M., Varghese, B.J., Shimokawa, H., Azuma, M., Ohya, K. and Ohyama, K. (2004) The deficiency of immunoregulatory receptor PD-1 causes mild osteopetrosis. *Bone*, 35, 1059–1068.
31. Dempster, D.W., Compston, J.E., Drezner, M.K., Glorieux, F.H., Kanis, J.A., Malluche, H., Meunier, P.J., Ott, S.M., Recker, R.R. and Parfitt, A.M. (2013) Standardized nomenclature, symbols, and units for bone histomorphometry: a 2012 update of the report of the ASBMR Histomorphometry Nomenclature Committee. *Journal of Bone and Mineral Research*, 28, 2–17.
32. Baker, M. (2016) Statisticians issue warning over misuse of *P* values. *Nature*, 531, 151.
33. Yaddanapudi, L.N. (2016) The American Statistical Association statement on *P*-values explained. *Journal of Anaesthesiology, Clinical Pharmacology*, 32, 421–423.
34. Pittman, J.W., Navalgund, A., Byun, S.H., Huang, H., Kim, A.H. and Kim, D.G. (2014) Primary migration of a mini-implant under a functional orthodontic loading. *Clinical Oral Investigations*, 18, 721–728.
35. Abraham, S. and Paul, M.C. (2013) Micro implants for orthodontic anchorage: a review of complications and management. *Journal of Dental Implants*, 3, 165–167.
36. Iijima, M., Takano, M., Yasuda, Y., Muguruma, T., Nakagaki, S., Sakakura, Y., Ochi, M. and Mizoguchi, I. (2013) Effect of the quantity and quality of cortical bone on the failure force of a miniscrew implant. *European Journal of Orthodontics*, 35, 583–589.

37. Lee, N.K. and Baek, S.H. (2010) Effects of the diameter and shape of orthodontic mini-implants on microdamage to the cortical bone. *American Journal of Orthodontics and Dentofacial Orthopedics*, 138, 8.e1–8; discussion 8.
38. Johnson, T.B., Siderits, B., Nye, S., Jeong, Y.H., Han, S.H., Rhyu, I.C., Han, J.S., Deguchi, T., Beck, F.M. and Kim, D.G. (2018) Effect of guided bone regeneration on bone quality surrounding dental implants. *Journal of Biomechanics*, 80, 166–170.
39. Furuya, Y., *et al*. (2013) Stimulation of bone formation in cortical bone of mice treated with a receptor activator of nuclear factor-kappaB ligand (RANKL)-binding peptide that possesses osteoclastogenesis inhibitory activity. *Journal of Biological Chemistry*, 288, 5562–5571.